Standing Mobility Device With Passive Lower Limb Exoskeleton for Upright Locomotion

Yosuke Eguchi, Hideki Kadone, and Kenji Suzuki, *Member, IEEE*

***Abstract*—This study proposes a novel standing mobility device aimed at supporting and assisting people with disabled lower limbs. The developed mobility device is capable of assisting voluntary postural transition between standing and sitting by a passive exoskeleton equipped with gas springs, in addition to providing wheeled locomotion in a standing posture using two in-wheel motors. The device allows voluntary natural assisted sit-to-stand motions. Furthermore, it can be operated in the standing posture without using hands. This paper describes the development and assessment of the standing mobility device as well as a pilot study conducted with a person with spinal cord injury. Then, investigation of the mechanical characteristics of the device is presented for further analysis of sit-to-stand and stand-to-sit transfer assistance.**

***Index Terms*—Assistive robotics, behavior-based systems, mechanism design, wheeled robots.**

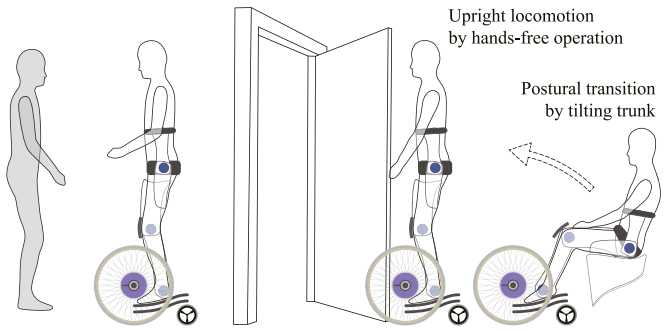

Fig. 1. Usage examples of developed standing mobility device (SMD). The SMD allows a user with lower limb motor disability to sit down, stand up as per his/her intention, and locomote in an upright posture by hands-free operation. These functions support essential motions in daily life, contributing to enhancement and diversification of the user's social activities.

I. Introduction

AROUND the world, there are a large number of wheelchair users with permanent disability in their lower limbs. For example, about 270,000 patients with spinal cord injury (SCI) in the U.S. have reduced motor function in the affected limb. Almost 40% of these patients received the injury in traffic accidents, and the average age at injury was 41.0 years [1]. Many of these patients were injured in their younger years. However, apart from wheelchairs, there are only a few options to supplement the mobility of SCI patients, which is essential for their social life. Thus far, various systems have been developed for people with SCI. These systems are, the wearable robot suit HAL [2], powered lower limb exoskeletons such as Ekso (Ekso Bionics, Freiburg im Breisgau, Germany) [3], Indego (Parker Hannifin, Cleveland, OH, USA) [4], ReWalk (ReWalk Robotics, Inc., Marlborough, MA, USA) [5] for rehabilitation, a passive gravity-balancing knee-ankle-foot orthosis [6], and a standing-style locomotion system [7]. However, few robotic systems such as REX [8], have been developed for assisting the daily locomotion of people with disabled lower limbs.

Patients on wheelchairs are constrained to the sitting posture, which causes inconvenience in their social life because almost all social environments are designed for able-bodied people who are capable of standing. In addition, the sitting posture makes it difficult for these patients to communicate with others by using gestures because of the difference in viewpoints and upper body heights [9]. Furthermore, wheelchair users cannot use their hands while they are moving because operation of a wheelchair requires at least one hand. The standing posture has medical benefits with regard to bone metabolism, the circulatory system, prevention of infections and inflammatory responses to the urinary tracts, as well as mental benefits such as greater independence [10]. Considering these points, a control method of a wearable robot for the sit-to-stand and stand-to-sit transfers of a complete SCI patient [11], devices for assisting the stand-up motion for rehabilitation [12]–[14], and an assistive device for the sit-to-stand transfer based on passive gravity compensation [15] were developed. Some upright wheelchairs and mobility aids were also developed, such as LEVO (LEVO AG) [16], Superior (Superior Sweden AB) [17], UPnRIDE (UPnRIDE

Manuscript received April 12, 2017; revised July 26, 2017 and October 23, 2017; accepted January 2, 2018. Date of publication May 18, 2018; date of current version August 14, 2018. Recommended by Technical Editor H. A. Varol. This work was supported in part by the Funding Program for World-Leading Innovative R&D on Science and Technology (FIRST Program), World leading human-assistive technology supporting a long-lived and healthy society, and in part by the Japan Society for the Promotion of Science KAKENHI under Grant 17H01251. *(Corresponding author: Hideki Kadone.)*

Y. Eguchi is with the Graduate School of Systems and Information Engineering, University of Tsukuba, Tsukuba 305-8577, Japan (e-mail: yosuke@ai.iit.tsukuba.ac.jp).

H. Kadone is with the Center for Innovative Medicine and Engineering, and Center for Cybernics Research, University of Tsukuba, Tsukuba 305-8577, Japan (e-mail: kadone@md.tsukuba.ac.jp).

K. Suzuki is with the Faculty of Engineering and Center for Cybernics Research, University of Tsukuba, Tsukuba 305-8577, Japan (e-mail: kenji@ieee.org).

Color versions of one or more of the figures in this paper are available online at http://ieeexplore.ieee.org.

Digital Object Identifier 10.1109/TMECH.2018.2799865

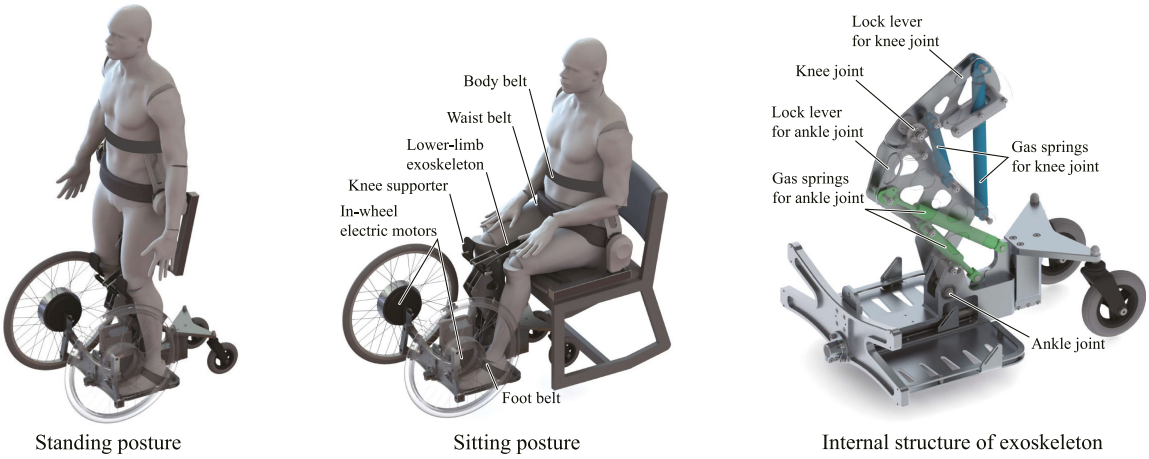

Fig. 2. Outline drawing of developed SMD and internal structure of exoskeleton. The SMD consists of a passive exoskeleton and electrically driven wheels. The exoskeleton consists of two pairs of gas springs to assist the motion of the ankle and knee joints. The exoskeleton assists a user in sit-to-stand and stand-to-sit postrual transition as well as in maintaining the standing posture. It also works as an interface to infer a user's intention of locomotion according to the tilting angle of the trunk during wheeled locomotion. The knee pad is used to fix the anteroposterior position of the knee joint of the user to align it with the knee of the exoskeleton.

Robotics Ltd., Yokne'am Illit, Israel) [18], and TekRMD (Matia Robotics, Inc., Salt Lake City, UT, USA) [19].

A personal mobility vehicle (PMV), which is a newly emerging transportation system for individuals, affords mobility functions that can be placed between walking and those of existing vehicles such as automobiles, motorbikes, and bicycles [20]; examples of PMVs include Segway PT (Segway, Inc., Bedford, NH, USA) [21] and Winglet (Toyota Motor Corp., Tokyo, Japan) [22]. These PMVs provide mobility in an upright posture with high controllability. However, they are designed for able-bodied people that are capable of standing without assistance.

In this study, we propose a novel device that provides high mobility in an upright posture for people with disabled lower limbs. In comparison to the above devices, the novelty of the device is that the exoskeleton provides natural sit-to-stand postural transition based on human biomechanics. It provides postural transition in accordance with anteroposterior tilting of the trunk by a compact mechanism consisting of passive springs and a link structure without using electric actuators.

Target users of this device are SCI people with control of the trunk, because their social independence can be greatly improved through provision of support for their lower limb functions. Fig. 1 shows the expected usage of the developed standing mobility device (SMD). The developed SMD consists of a wearable passive exoskeleton and wheels driven by electric motors (see Fig. 2). The exoskeleton assists a user with postural transitions between sitting and standing and with maintaining either of these postures. The user is able to execute upright locomotion by driving the electric wheels using the trunk orientation as a control interface. Consequently, the SMD facilitates diverse activities such as using a vending machine; passing through, opening, and closing a door; and using a shelf designed for use in a standing posture. Furthermore, the SMD enables the user to communicate with other people using gestures during locomotion, providing an even viewpoint at a comparable height.

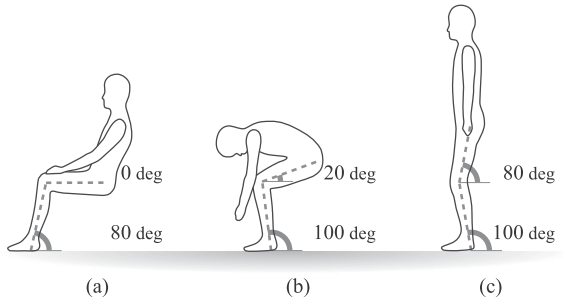

Fig. 3. Model of inter-postural transition and attitude of lower limbs. The model has three phases—sitting, intermediate, and standing postures—to achieve safe and smooth transition between postures. (a) Sitting posture. (b) Intermediate posture. (c) Standing posture.

Overview of the mechanical design of the SMD has been reported in [23]. This paper presents a detailed method for structuring the SMD including determination of the attachment position and size of the gas springs. Moreover, it presents actual measurement of generated joint moment, and experiments investigating its feasibility with healthy and SCI participants to prove the performance of the developed prototype.

II. Approach

A. Postural Assistance

This research aims to provide assistance with natural inter-postural transitions by a small, lightweight, and easy-to-wear exoskeleton system. This system enables controlled inter-postural transitions according to anteroposterior shifting of the upper body. Although electromyography may also be a candidate for a control interface, it is difficult to be applied on the lower limbs of complete SCI patients with very low activation potential [11].

In an analysis of standing up motion of a healthy participant (age 23 years, 180 cm) using a motion capture system (MAC3D, Motion Analysis Co., Ltd., Santa Rosa, CA, USA),

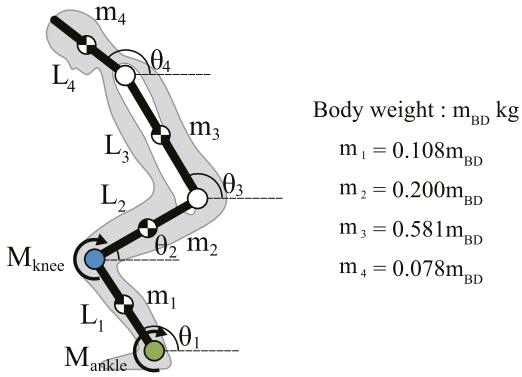

Fig. 4. Four-link model used to calculate moment on each joint. $L_i (i = 1, 2, 3, 4)$ denote the lengths of the shank, thigh, trunk, and head-neck segments, respectively. m_i denote the mass of each part of the body, which is obtained by using the entire body weight m_{BD} and the body parts mass index. θ_i is the sagittal angle of each limb against the horizontal plane.

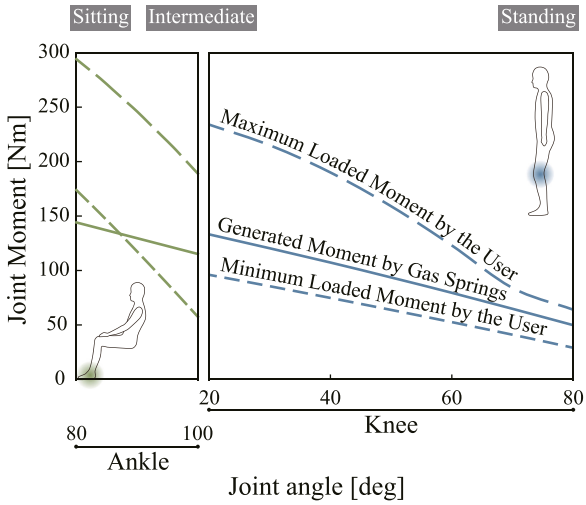

Fig. 5. Relationship between the moment loaded by the user's weight and the moment generated by the gas springs, for the ankle joint (left) and for the knee joint (right). The condensed broken lines represent the minimum loaded moment (when the participant kept the trunk bended anteriorly); the broken lines represent the maximum loaded moment (when the trunk was aligned with the vertical). Those are estimated using (1a) and (1b). The solid lines represent the moment generated by the gas springs. They are estimated using (4) with a specific configuration for the participant's height and weight. The moments are plotted in their absolute value.

it was observed that the ankle, knee, and hip joints are moved in coordination in the sagittal plane. Since the standing transition can be represented by the motion of these three joints, we consider designing the exoskeleton such that it has joints corresponding to these three joints in the human body. To avoid large acceleration or velocity, which may lead to falling, we employ a passive actuation system that maintains its posture close to static equilibrium all through the postural transition.

To assist postural transition in a manner such that it remains similar to normal transition, we first model the inter-postural transition. We then calculate joint moments that realize equilibrium against gravitational force at each instant of transition. Finally, we design the exoskeleton according to the required moment.

1) Postural Transition Model: This model includes the standing, sitting, and intermediate postures (see Fig. 3).

In the sitting posture [see Fig. 3(a)], the shank should stay outside of the space below the hip so that a user can sit on a normal chair. For this reason, the shank is defined to be inclined 10° posteriorly. In the standing posture [see Fig. 3(c)], to ensure smooth start of postural transition, the moment in the knee joint should be loaded in the flexion direction. For this reason, the thigh is defined to be inclined 10° posteriorly and the shank inclined 10° anteriorly, relative to the vertical. In this posture, the center of gravity of a user's body is within the supporting area. In addition, an intermediate posture [see Fig. 3(b)] is defined for simplifying the motion of the knee and ankle joints. The knee joint stays fixed during transition between the sitting (a) and intermediate (b) postures, and the ankle joint stays fixed during transition between the intermediate (b) and standing (c) postures. Furthermore, it is considered that the upper body should not be tilted posteriorly beyond the vertical without supporting material on the back, so as not to cause discomfort to the user.

2) Calculation of Joint Moment: The mass of each body segment m_i is estimated by Matsui's body parts mass index [24] according to the actual entire body mass m_{BD} (see Fig. 4). These estimated values are then used for computing the moment on an ankle joint (M_{ankle}) and a knee joint (M_{knee}). The center of gravity of each limb is assumed to be located at the lengthwise center.

$$M_{\mathrm{ankle}} = \left(\frac{1}{2}m_1 + m_2 + m_3 + m_4\right) gL_1 \cos\theta_1 + M_{\mathrm{knee}} \tag{1a}$$

$$M_{\mathrm{knee}} = \left(\frac{1}{2}m_2 + m_3 + m_4\right) gL_2 \cos\theta_2 + \left(\frac{1}{2}m_3 + m_4\right) gL_3 \cos\theta_3 + \frac{1}{2}m_4 gL_4 \cos\theta_4 \tag{1b}$$

where m_i, L_i, and θ_i denote the mass, length, and sagittal angle, respectively, against the horizontal of each body segment (see Fig. 4). Equations (1a) and (1b) give the static moment acting at the ankle and knee joints, respectively.

3) Exoskeleton Design: The static moments loaded by a user's weight on his/her anatomical joints (M_{load}) are calculated using (1a) and (1b) for each posture through the postural transition defined in Section II-A1. The loaded moment varies depending on the tilting of the upper body. When the upper body is bent to the anterior limit, the moment is minimum (M_{min}). When the upper body is aligned with the vertical, which is the posterior limit according to the postural transition model, the maximum moment (M_{max}) is loaded on each joint. Fig. 9 shows the temporal profile of each joint angle when a healthy participant (age 23 years, 180 cm, 70 kg, $L_1 = 40$ cm, $L_2 = 47$ cm, $L_3 = 50$ cm, and $L_4 = 30$ cm) performed postural transition from standing to sitting. Here, the participant was asked to bend his trunk and head anteriorly as much as possible while maintaining natural movement. This profile is used for calculating the minimum loaded moment. Fig. 5 (left) shows the minimum (con-

densed broken line) and maximum (broken line) moments on the ankle joint for each posture during transition between the sitting and intermediate postures, whereas Fig. 5 (right) shows those for the knee joint during transition between the intermediate and standing postures. These are computed using (1a) and (1b).

The design strategy of the exoskeleton mechanism is such that the assisted postural transition can be controlled by the user's anteroposterior tilting of the trunk. During postural transition, the M_{load} discussed above is acting as flexor moment in the direction of stand-to-sit. At the same time, the force of the springs is acting through the link structure as extensive moment around the joints of the user in the direction of sit-to-stand. We refer to this moment as *generated moment* (M_{gen}) and discuss more precisely later in this section. By the natural mechanics, the direction of the assisted postural transition depends on the magnitude relationship between M_{load} and M_{gen}. The transition is in the stand-to-sit direction when $|M_{\mathrm{load}}|>|M_{\mathrm{gen}}|$, and sit-to-stand direction when $|M_{\mathrm{load}}|<|M_{\mathrm{gen}}|$. For the user to be able to control the direction by anteroposterior tilting of the trunk, M_{gen} should be designed to fulfill

$$|M_{\mathrm{min}}| < |M_{\mathrm{gen}}| < |M_{\mathrm{max}}| \tag{2}$$

in terms of the possible mimimum and maximum loaded moment according to the trunk tilting. By this way, the user can induce assisted sit-to-stand postural transition by tilting the trunk anteriorly, and stand-to-sit transition by tilting posteriorly. The moment relationship of (2) is defined as Requirement 1. In addition, at the initiation of sit-to-stand transition in sitting posture, to make sure that the initiation occurs in accordance with apparent intension of the user, pushing the seat surface by the upper limb is designed to be required, therefore M_{gen} should fulfill $|M_{\mathrm{gen}}|<|M_{\mathrm{min}}|$ at this moment. This is defined as Requirement 2.

In the first step of the exoskeleton design, the basic geometry of the link structure is defined so that it fits to the segment length and joint center position of the lower limb anatomy of a specific user (see Fig. 6). It is designed strictly compact to be placed between the lower limbs. A rectangular area in which an end of a spring can be attached without interfering with the internal structure of the exoskeleton is defined for each of the ends. Then, the question now is to determine the specifications of a gas spring and its position to be attached on the link structure. This is a multiple factor exploration problem pertaining to the maximum/minimum length, reaction force characteristics against compression, attachment positions of the movable and base ends, joint angle range and joint moment characteristics when attached on the link structure. To automate the procedure we implemented the following algorithm. It checks the validity of spring characteristics in terms of (a) geometric validity, (b) range of joint movement, and (c) joint moment characteristics, for all the allowed combination of the attachment position of the spring ends, in the end to obtain sets of valid springs and their attachment positions.

a) *Geometric validity:* A list of available gas springs is defined, for example using product catalogs. The springs whose length is out of range for fitting into the exoskeleton are removed from the list. To fit into the exoskeleton, the length and compression range of a spring have to fulfill the conditions.

i) The shortest distance between the base and movable ends ($|A-B|$) must be shorter than the maximal length of the gas spring.

ii) The longest distance between the base and movable ends ($A+B$) must be longer than the minimal length of the gas spring.

A and B are the distance from the joint rotation center to the movable end and to the base end, respectively, (see Fig. 6).

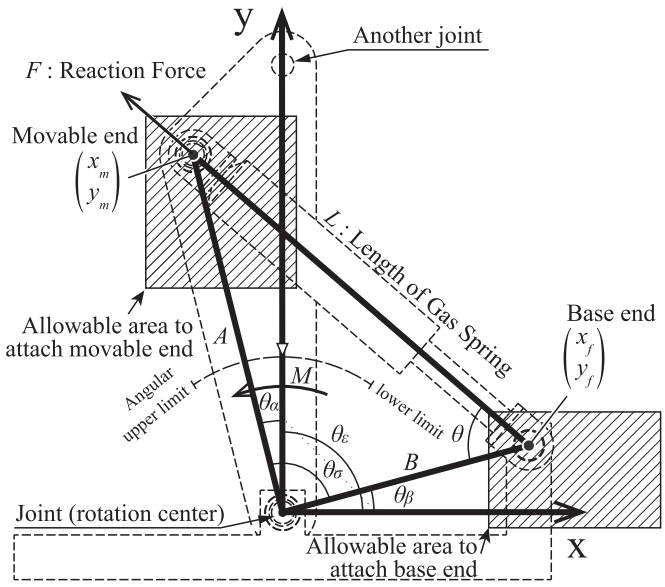

Fig. 6. Geometric definition for designing the arrangement of gas springs. The coordinate origin is set at the rotation center of the joint. A line that connects the joint to the next joint is aligned with the *Y*-axis for convenience. Rectangular shapes indicate the areas in which the base and movable ends of the gas spring can be attached to the links.

b) *Range of joint movement:* The movable range of joint angle θ_ϵ of the exoskeleton needs to be able to cover the motion range of the corresponding anatomical joint angle defined by the postural transition model; 80 to 100° for the ankle and 20 to 80° for the knee (see Fig. 3). The list of springs is truncated by the conditions.

i) When the gas spring is at its minimum length, θ_ϵ must be smaller than the minimum anatomical joint angle achieved during the transition movement.

ii) When the gas spring is at its maximum length, θ_ϵ must be greater than the maximum anatomical joint angle achieved during the transition movement.

The joint angle θ_ϵ is calculated as

$$\theta_\epsilon = \theta_\beta + \theta_\sigma - \theta_\alpha \tag{3}$$

where θ_β, θ_σ, and θ_α denote, respectively, the angle between line B and the *X*-axis, the angle between lines A and B, and the angle between line A and a line that connects the joint to another joint in the figure, which are computed by planar trigonometry.

c) *Joint moment characteristics:* The moment M generated by the gas spring on the joint is

$$M = BF\sin(\theta) \tag{4}$$

where F denotes the reaction force of the gas spring at length L, and θ denotes the angle between line B and the axial direction of the gas spring. $M_{\rm gen}$ is equivalent to M minus the moment originating from the mass of the exoskeleton. The spring list is truncated by the requirements on the moment relationship.

i) $|M_{\rm min}| < |M_{\rm gen}| < |M_{\rm max}|$, for the ankle joint at the intermediate posture [see Fig. 3(b)], and for the knee joint at each posture between the intermediate and the standing postures [see Fig. 3(c)] (Requirement 1).

ii) $|M_{\rm gen}| < |M_{\rm min}|$, for the ankle joint at the sitting posture [see Fig. 3(a)] (Requirement 2).

B. Locomotion Assistance

Most powered wheelchairs are joystick controlled. However, even during locomotion, upper limbs have significant functions such as handling objects and making gestures for communicating with others. Although previous works [25], [26] have revealed that an electric wheelchair could be controlled on the basis of the electroencephalogram, this remains a topic of further research because the inference of intention takes several seconds. In this regard, we propose a real-time control interface of the SMD based on the voluntary postural change of the upper body.

First, the attitude of a user's trunk is inferred according to the joint angle of the exoskeleton segments (see Fig. 8):

$$\theta_B = \gamma \left(\frac{\theta_R + \theta_L}{2} - \theta_\gamma \right) \tag{5}$$

$$\theta_T = \delta \tan^{-1} \left(\frac{L_A \left(\cos\theta_L - \cos\theta_R \right)}{W_B} \right) \tag{6}$$

where θ_B and θ_T are the tilting and torsion angles, respectively, of the trunk (anterior tilting and counterclockwise torsion are defined as positive); and θ_R and θ_L are the orientation angles of the exoskeleton segments attached to the right and left sides, respectively, of a user's trunk. These are measured against the horizontal plane. L_A denotes the length of the exoskeleton segment from the fixing point on a user's trunk to the rotation center, W_B denotes the width of a user's trunk, γ and δ are adjusting coefficients to correct inferred angle to approximate real angle, and θ_γ is a constant that accounts for the offset between a user's trunk tilt angle at his/her natural upright posture and the vertical axis in the sagittal plane.

Then, the control values of velocity υ and angular velocity ω of the SMD are calculated in proportion to the inferred trunk attitude (θ_B and θ_T, respectively).

$$\upsilon = \alpha\theta_B \tag{7}$$

$$\omega = \beta\theta_T. \tag{8}$$

The parameters $\alpha, \beta, \gamma, \theta_\gamma$, and δ are determined experimentally. The SMD is controlled with low acceleration to avoid instability in the forward and backward directions.

III. System Configuration

Locomotion in the upright posture and voluntary postural changes between the standing and sitting postures are achieved by a combination of a passive exoskeleton system and electrically driven wheels. Fig. 7 shows sequential images of the assisted inter-postural transition.

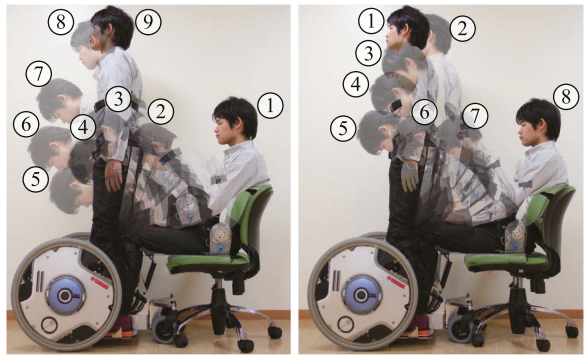

Fig. 7. Motion of inter-postural transition using the developed exoskeleton. The numbers represent the sequence of motion. Asymmetricity of the two motions is observed. The trunk is bent anteriorly during the sit-to-stand transfer and posteriorly during the stand-to-sit transfer.

TABLE I
Specification of the SMD

Dimension [cm]	Width 66 Length (Standing) 85 (Sitting) 114 Height (Standing) 133 (Sitting) 91 Wheel base (Max.) 58 (Min.) 49 Tread (F) 56 (R) 25
Mass [kg]	36.8
Gas Springs	KYB FLF125-50 (Max. 479mm, 490N) KYB FLF75-50 (Max. 362mm, 490N) 2 x KYB KPG50-80 (Max. 209mm, 785N)

A. Hardware

The developed SMD consists of the passive exoskeleton system that we call a passive assistive limb, which assists a user in changing and maintaining posture, and the electrically driven wheels, which carry the structures. The specifications of the SMD are listed in Table I, and the internal structure of the exoskeleton is shown in Fig. 2 (right).

Each of the ankle and knee joints of the exoskeleton is driven by a pair of gas springs which generate moment at the joint. The exoskeleton itself does not have any electric actuator to generate joint moments and therefore it does not need neither computerized controller nor power source. The characteristics allow the exoskeleton to be lightweight and compact enough to fit between the legs. Length of a gas spring can be fixed or freed by operating a lock lever. When a spring is locked, the corresponding joint of the exoskeleton is locked. In addition, the exoskeleton is equipped with foot belts, knee supporters, a waist belt, and a body belt for fixing it on a user (see Fig. 2).

B. Control System

Electric control system is implemented with the SMD for hands-free wheeled locomotion (see Fig. 8). The angles of the ankle, knee, and hip joints of the exoskeleton are acquired

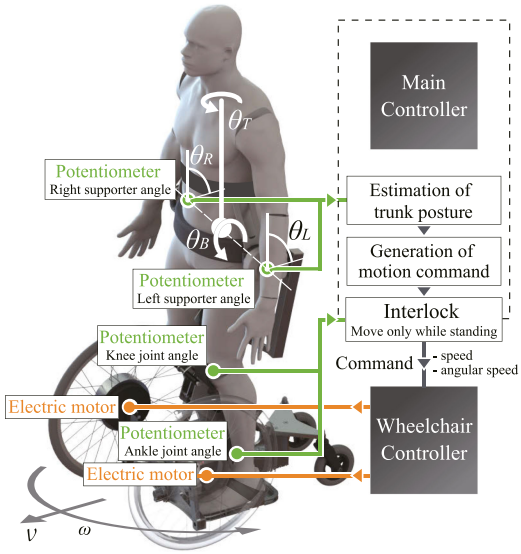

Fig. 8. Configuration of control system for upright locomotion. Angular data of the ankle, knee, and supporters around the hip joint are transmitted to the main controller. The controller estimates the trunk posture by the angles and sends the target values of velocity and angular velocity to the electric wheelchair controller for hands-free operation.

through embedded potentiometers, and the control values are computed by (5)–(8). The main controller operates an electric power unit for wheelchair (JWX-1, YAMAHA Motor Corp., Iwata, Japan) by sending the control values to it. Its control circuit is modified to accommodate control commands not only from its original joystick but also from an external source for controlling the forward/backward velocity and angular velocity. The SMD can be moved forward and backward, as well as turned, by controlling the pair of the in-wheel electric motors. The hands-free operation system realizes real-time control just like the original joystick. The parameters in (5)–(8) are determined experimentally as $\alpha = \beta = 571, \gamma = \delta = 1$, and $\theta_\gamma = 1.57$.

The hands-free operation is automatically disabled when the exoskeleton is not in standing position. This is judged by the values of the potentiometers attached at the ankle and knee joints of the exoskeleton. Also, a user can manually disable the hands-free operation whenever he/she wants. It allows him/her to enjoy communicating with others using gestures or to reach out to things without caring about unintentional motion of the SMD.

C. User Operation

Following the implementation, a typical user operation of the SMD can be summarized as follows. In a sitting position, a user starts the operation by freeing the lock lever for the ankle joint. The user initiates the stand-up motion by pushing the seat surface by hands as well as tilting the trunk anteriorly to reach the intermediate posture, where the user operates the lock levers to lock the ankle joint and free the knee joint. Then by tilting the trunk anteriorly, stand-up motion of the knee joint is performed, and the user reaches a standing posture, where the user locks the knee joint. In the standing posture, the user can navigate around the environment by driving the electric wheels using the hands-free controller interface. When the user wants to sit down, the user frees the knee joint, tilts the trunk posteriorly to reach the intermediate posture, locks the knee joint and frees the ankle joint, tilts the trunk posteriorly to reach a sitting position, and locks the ankle joint.

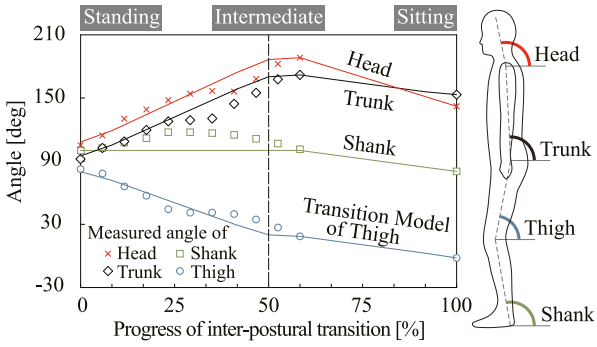

Fig. 9. Measured and modeled segment attitude during postural transition. Each dot and line represents respectively the measured and modeled angle of a body segment against the horizontal at each instant through stand-to-sit transition without using the device.

IV. Experimental Validation

All the experiments with subjects were reviewed by the institutional review board of University of Tsukuba or University of Tsukuba Hospital. Written informed consent was obtained from the participants.

A. Natural Postural Transition

An experiment was conducted for investigating the inter-postural transition model described in Section II-A1. The angles of the shank, thigh, trunk, and head-neck segments against the horizontal were measured during postural transition without the device. The attitude transition of each limb during transition is shown in Fig. 9. In this figure, the postures at 0, 50, and 100% correspond to the postures (c), (b), and (a), respectively, of Fig. 3. Since it was difficult to maintain quasi-static posture at some points between intermediate and sitting posture, the obtained angle data on latter half is less than that of the first half. The transition model is defined by piecewise linear interpolation of the sampled points so that it monotonically increases or decreases (marked as the *transition model* in the figure) including the standing, intermediate, and sitting postures described in Section II-A1. A difference of up to 20° is observed between the model and the real transition. This difference is attributed to the motion of maintaining balance in an approximately quasi-static transition without using the device.

B. Measurement of Joint Moment on Exoskeleton

The moment generated by the gas springs on the joints of the exoskeleton was measured with the aim of investigating its mechanical characteristics. A towing hook was attached to the exoskeleton to connect a steel wire that would induce a moment on the joints by pulling. Then, each joint angle was measured by a built-in potentiometer, and the corresponding tension of the

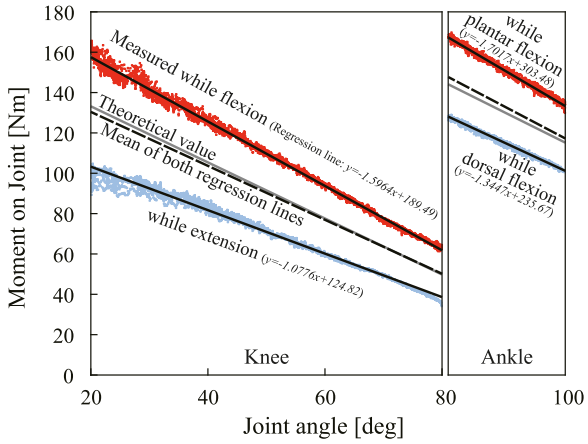

Fig. 10. Measured moment on each joint of exoskeleton. The red and blue dots represent result of five measurement trials of the moment while the gas spring is shrunk and elongated, respectively. The gray lines represent the theoretical moment generated by ideal frictionless gas springs. A black line represents the regression line for each measured data series, and the broken lines indicate the average of the two black lines.

wire was measured by a force gauge (ZP-1000N, IMADA Co., Ltd., Toyohashi, Japan). Finally, the moment on each joint was calculated using a geometrical relationship of the exoskeleton. Meanwhile, the angular velocity of each joint was kept low enough to approximately realize quasi-static state.

Measurement results on the knee joint and ankle joint are shown on the left and right side, respectively, in Fig. 10. The average of the generated moment on the ankle joint during plantar flexion motion was 16% greater than the theoretical value and that on the knee joint during flexion motion was 18% greater as well. During these motions, the gas springs are compressed. Similarly, the average of the generated moment on the ankle joint during dorsal flexion motion was 11% smaller than the theoretical value and that on the knee joint during extension was 24% smaller as well. During these motions, the gas springs are lengthened. One reason for this is the asymmetric property of the reaction force of the springs caused by friction on the slide members. The average of the generated moment was 2% greater on the ankle joint and was 3% smaller on the knee joint than the theoretical value.

C. User's Weight and Height That Are Compatible With the Developed Exoskeleton

While the developed exoskeleton is designed to be compatible with users of a specific weight and height, it is expected that some difference in weight and height can be allowed. Weights and heights that are compatible with the specifications of the developed exoskeleton were investigated. The following algorithm generates parameter sets of a body model, estimates joint moments and judges if each set of the parameters is compatible with the device.

1) *Generation of weight parameters for body model:* A set of various body weight parameters is generated by sampling from the designated weight range with a 1 kg interval. For each sample, the weights of the shank, thigh, trunk/hand, and head/neck segments are calculated using Matsui's body parts mass index [24].
2) *Generation of height parameters for body model:* A set of various body height parameters is generated by sampling from the designated height range with a 1 cm interval. For each sample, the lengths of the shank, thigh, trunk, and head-neck segments are calculated by referring to the average body segment ratio extracted from the AIST/HQL Database of Human Body Dimension and Shape 2003 [27].
3) *Configuration of postural transition model:* In this step, standup motion, which follows the sitting, intermediate, and standing postures, with maximum anterior bending of the upper body is configured. In the same manner, sit-down motion, which reversely follows the stand-up motion while aligning the upper body with the vertical, is configured.
4) Estimation of generated joint moment: Joint moments applied by the exoskeleton system to a user's body are calculated for each posture.
5) *Estimation of loaded joint moment:* Every combination of body weight and height is applied to the four-link model (see Fig. 4), and joint moments applied by a user's body are calculated for each posture.
6) *Judgment on the compatibility of each weight and height with the developed device:* The combination of the body weight and height has to fulfill all of the following requirements on the magnitude relationship of the generated and loaded moments.

For the ankle joint,

a) $|M_{\mathrm{gen}}| < |M_{\mathrm{max}}|$ for each posture during the sit-down motion (Requirement 1, Section II-A3).
b) $|M_{min}| < |M_{\mathrm{gen}}| < |M_{\mathrm{max}}|$ at the intermediate posture (Requirement 1).
c) $|M_{\mathrm{gen}}| < |M_{\mathrm{min}}|$ in sitting position (Requirement 2).

For the knee joint,

d) $M_{\mathrm{min}}| < |M_{\mathrm{gen}}| < |M_{\mathrm{max}}|$ for each posture between the intermediate and standing postures (Requirement 1).

Simulation results for the developed exoskeleton are shown in Fig. 11. The gray-colored domain shows the weight and height that is compatible with the exoskeleton, as obtained on the basis of the actual measured moment described in Section IV-B; the light-gray-colored domain shows the corresponding range for the same exoskeleton but with ideal frictionless springs. Limitation on the weight depends on the generated joint moment and the body height. On the other hand, limitation on the height depends on the length of the shank part of the exoskeleton because the length of the part is not adjustable. As a result, it is confirmed that more than 20 kg of body weight variation can be accommodated by the developed device. The filled circles in Fig. 11 show the weight and height of the participants of the experiment described in Sections IV-E. Even though two of the participants were out of the domain, all participants were able to perform postural transition with the support of the exoskeleton. Since the simulation considers only quasi-static equilibrium on the joint moment, it can be potentially explained by the dynamic motion of the trunk that induces a moment on each joint.

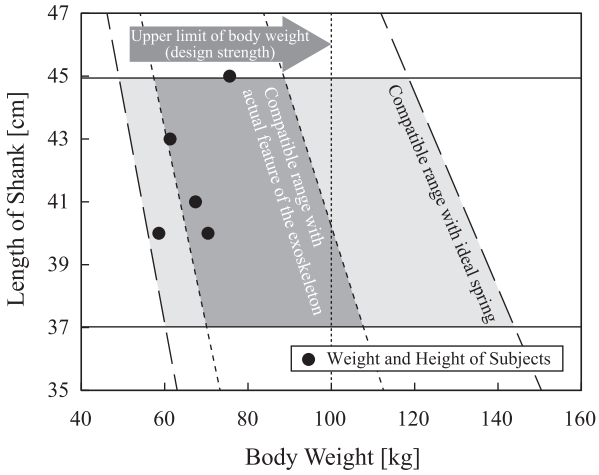

Fig. 11. Range of weight and height compatible with the exoskeleton. Ranges of compatible weight and height are indicated for ideal frictionless springs (light-gray) and for actual mechanical characteristics of the exoskeleton (gray).

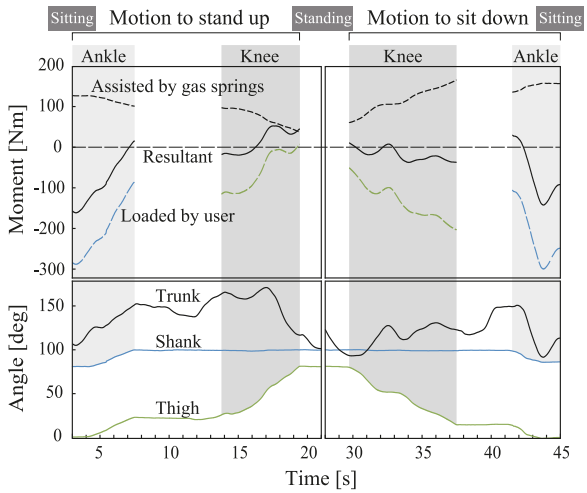

Fig. 12. Limb segment attitude and joint moment during postural transition. The left part shows stand-up motion, and the right part shows sit-down motion. The lower part shows the attitude of each body segment, and the upper part shows the moment on each joint, estimated from the attitude and body weight.

D. Pilot Study of Postural Transition With Healthy Participant

A pilot test with a healthy participant (age 23 years, 180 cm, 72 kg) was conducted to evaluate the magnitude relationship between assistive moment generated by the gas springs and the moment loaded by the user during postural transition. Here the participant was asked to keep the transition speed low to approximate quasi-static states. It was observed that after a few trials the participant could change his posture as expected by anteroposterior tilting of the upper body. No comment was reported relating to discomfort caused by the force applied by the exoskeleton.

Attitudes of the shank, thigh, trunk, and head-neck segments were measured using a motion capture system (MAC3D, Motion Analysis Co., Ltd., USA) for verifying whether postural transition could be performed by weight shifting along with tilting of the trunk. The relationship between magnitudes of the moment generated by the gas springs and the moment loaded on the joints of the exoskeleton according to the posture of the participant was investigated (see Fig. 12). In the initial phase of standing up, the loaded moment on the ankle was greater than the generated moment. The participant pushed on the seat surface to initiate forward rotation around the ankle joint. Once the shank reached 100°, the loaded moment became smaller than the generated moment, and the participant maintained posture without support of hands. The loaded moment was almost balanced with the generated moment when the upper body was tilted anteriorly. Furthermore, the motion of sitting down commenced when the upper body was tilted posteriorly. The fluctuation of the trunk angle in 7–14 s and 37–42 s are due to the motion to handle the lock levers of the springs. Joint moment of this time period is not shown because the springs do not apply moments herein since the exoskeleton is rigid because the joints are locked. Through the motions, fluctuation of the trunk angle was used for adjusting the balance between the loaded and generated moments to enable intended motion at intended speed.

E. Required Time for Postural Transition With Assistance

Required time to perform postural transition may depend on user because of the use of the passive mechanism. Average required time and its deviation among users was investigated. Five healthy male participants (age 22.8 $\pm$ 1.9 years, 175.7 $\pm$ 4.4 cm, 66.7 $\pm$ 6.7 kg) were asked to perform postural transition at their natural speed with the assistance of the device. Operational procedure for postural transition using the device was shown to them once, and then they familiarized themselves with the device through several times of trial. During all that time, instructions were given when asked. Subsequently, the time required by each participant to perform the transition was measured three times. In this experiment, time required to stand up was defined as the time difference between the instant when the ankle joint was unlocked in the sitting posture and the instant when the trunk was aligned to the vertical in the standing posture. In the same manner, time required to sit down was defined as the time difference between the instant when the trunk was tilted posteriorly in the standing posture and the instant when the ankle joint was locked in the sitting posture. The average time required to stand up was 10.87 $\pm$ 2.82 s, and that to sit down was 9.67 $\pm$ 2.06 s. On the other hand, the time for normal transition without the device was 1.84 $\pm$ 0.26 s, and 1.91 $\pm$ 0.29 s, respectively. The required time for postural transition using the developed device is comparable to those of other systems with electric motors.

F. Evaluation of Assist for Postural Transition by Muscle Usage in Healthy Participants

To evaluate the motion assist by the developed device for sit-to-stand and stand-to-sit postural transitions, we conducted experiments with healthy participants to compare the necessary muscle activity with and without using the device.

Eight healthy participants (age 29.1$\pm$ 5.5 years, 174.5 $\pm$ 6.5 cm, 65.1 $\pm$ 7.3 kg) participated in the experiments. The

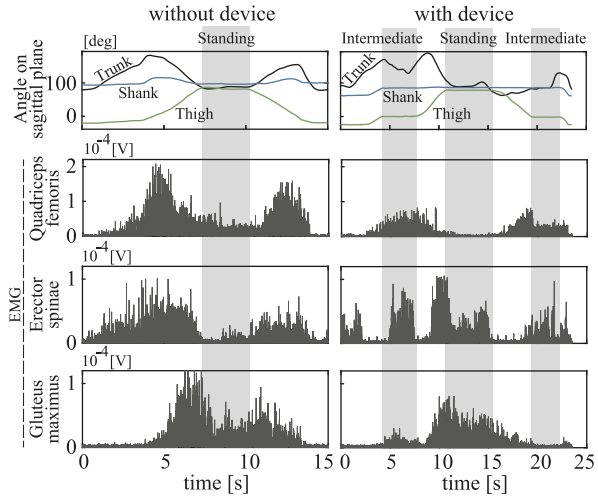

Fig. 13. Measured EMG data and body attitude of a participant while postural transition without (left) and with (right) the developed device. These EMG data are shown in absolute value after band-pass filtering.

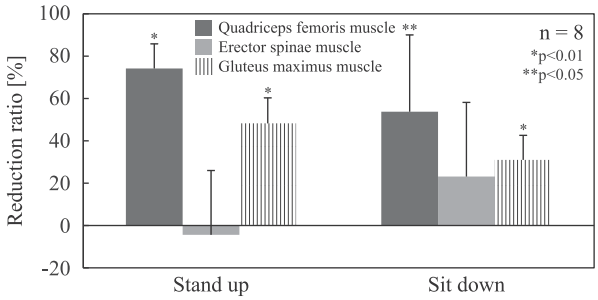

Fig. 14. Reduction ratio of maximum muscle activation during sit-to-stand (left) and stand-to-sit (right) postural transition using the developed device in comparison with the transition without using the device. Positive values show reduced maximum muscle activation in assisted transition in comparison with unassisted transition.

participants performed sit-to-stand and stand-to-sit postural transitions three times with using the device and then without using it. During the experiments, the participants were equipped with wireless Electromyography (EMG) sensors (Trigno Lab, Delsys, USA) on the bilateral extensor muscles; quadriceps (vastus medialis) for knee extension, erector spinae for trunk extension and gluteus maximus for hip extension. Markers of a motion capture system (MX System, Vicon Motion Systems, Ltd., U.K.) were attached on the Acromion, Great Trochanter, Lateral Epicondyle of Femur, and Lateral Malleolus to record sagittal motion in synchronization with the EMG, in order to detect the start and end of the transition motions (see Fig. 13). EMG data were band-pass filtered, rectified, and evaluated according to maximum value of local integration by a moving window of 100 ms width. A paired t-test was adopted to compare between the two conditions. In the assisted sit-to-stand case, maximum activation levels were reduced in average by 74.2% ($p < 0.01$) for quadriceps and 48.3% ($p < 0.01$) for gluteus maximus when compared to that of the unassisted case. In the assisted stand-to-sit case, they were reduced in average by 53.8% ($p < 0.05$) and 31.0% ($p < 0.01$) (see Fig. 14). On the other hand, the activation of erector spinae showed nonsignificant increase by 4.4% ($p > 0.1$) in sit-to-stand transition, and nonsignificant decrease by 23.1% ($p > 0.05$) in stand-to-sit transition. Here, the reduction ratio $R_{\mathrm{reduction}}$ of maximum muscle activation is calculated as

$$R_{\mathrm{reduction}} = \frac{-(\mathrm{EMG}_{\mathrm{with}} - \mathrm{EMG}_{\mathrm{without}})}{\mathrm{EMG}_{\mathrm{without}}} \quad (9)$$

where $\mathrm{EMG}_{\mathrm{with}}$ and $\mathrm{EMG}_{\mathrm{without}}$ are EMG value observed while postural transition with and without the developed device, respectively. Significantly reduced usage in the knee and hip extensor muscles during postural transitions using the device was observed in the healthy participants, indicating the possibility that patients with significant reduction in the lower limb muscle control might be able to perform the postural transitions using the device. On the other hand, the trunk extensor muscle did not show significant difference, which is reasonable since the device leaves the upper body free.

G. Pilot Study of Postural Transition With SCI person

The participant of this experiment was a male with incomplete SCI on T5-9. He was capable of generating torques on the lower limbs enough to make swing motion utilizing gravity while holding onto parallel bars and supporting body weight by his arms. Without using support of the arms, he was not capable of standing up, keeping standing posture, sitting down or walking. Effectiveness of the proposed method was investigated through assessment tests conducted with the participant. First, the participant was asked to familiarize himself with the device so that he was able to perform the entire operation of postural transition by himself. Then, he was asked to perform inter-postural transition with the support of the device. His motion was measured using a motion capture system (MX System, Vicon Motion Systems, Ltd., U.K.). As a result, it was found that performing the stand-up motion required 50 s and performing the sit-down motion required 14 s and that the participant was able to maintain his body in the standing posture by himself. The time required by the SCI person to perform the sit-down motion was almost the same as that required by the healthy participants (Section IV-E), whereas the time to perform the stand-up motion was much more than that required by the healthy participants. After the experiment, the participant commented that he first did not get an idea of which muscle to use for stabilizing the body but after getting familiarized with the device it was not an issue anymore. The comment suggested that it might be possible to further reduce the required time of postural transition by some more familiarization. We considered that the part that required familiarization the most was the timing to start raising the bended trunk up to the vertical in coordination with the knee extension. Fig. 15 shows the relationship between the generated and loaded moments on the knee joint while flexion/extension motion was performed between the intermediate and standing postures. The loaded moment was less than the generated moment while the knee joint was in extension motion; on the other hand, the loaded moment was greater than the generated moment while this joint was in flexion motion. This result implies that the developed system can help SCI patients by assisting them in stand-up and sit-down motions.

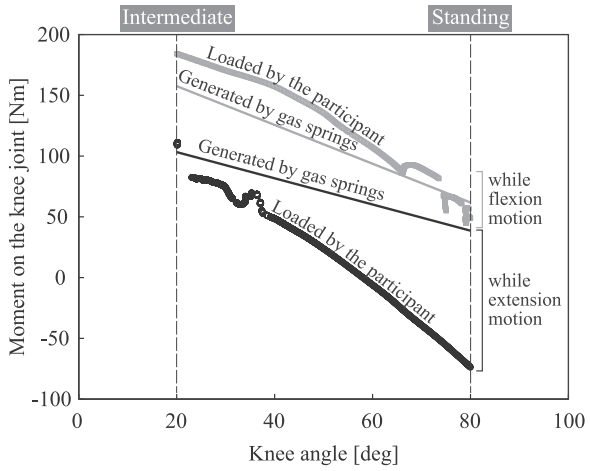

Fig. 15. Relationship between generated (extension direction) and loaded (flexion direction) moments on the knee joint in the assessment with SCI person. Each dot represents the loaded moment and the lines represent the generated moment. Direction of resultant moment can be read from positional relationship between a line and dots. If black dots are located under the black line, direction of resultant moment is extension direction on the joint because generated moment (extension) is greater than loaded moment (flexion).

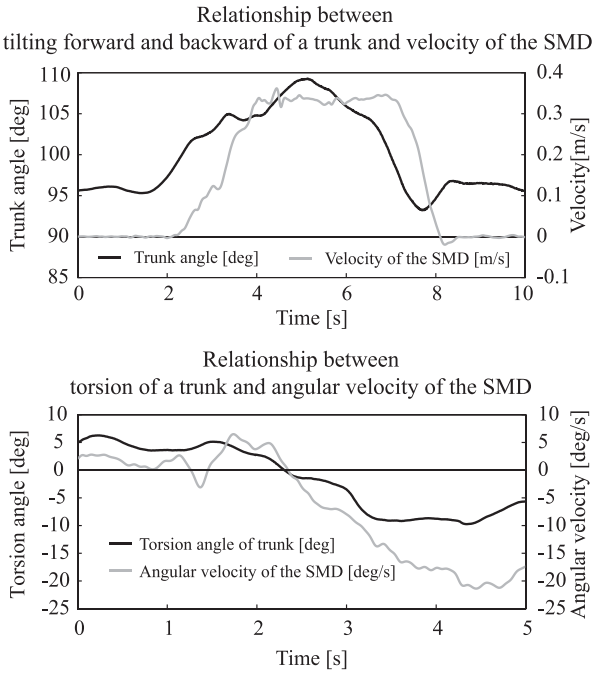

Fig. 16. Experimental results of locomotion assistance by the SMD. The attitude of a participant and the position, velocity and angular velocity of the SMD were measured and estimated using a motion capture system.

H. Locomotion Assistance

Locomotion in the upright posture controlled by the trunk attitude was examined with a healthy participant (age 23 years, 180 cm, 72 kg) using the developed SMD. For safety purposes, a walking aid was used in this experiment. The participant of the experiment was the same healthy person who participated in the experiment described in Section IV-D.

The participant could navigate the device in any direction by tilting his trunk. The speed and the attitudes of the SMD and the attitudes of the trunk were measured for evaluation using a motion capture system (MAC3D, Motion Analysis Co. Ltd., USA). Results of the experiment demonstrated that the motion control functioned appropriately according to the relative attitudes of the SMD and the trunk of the participant. The trunk attitude in the anteroposterior direction was calculated from a line segment between the seventh cervical spine and the sacrum. The attitude in the twist direction was calculated from a line segment between the right and left shoulders. The relationship between the anterior and posterior tilting of the trunk and velocity of the SMD is shown in the upper part of Fig. 16. The SMD was stationary in the initial phase, then accelerated according to the attitude of trunk, and finally stopped by the posterior tilting of the trunk. The lower part of Fig. 16 shows that the angular velocity of the SMD was controlled on the basis of the twist angle of the trunk.

V. Discussion and Conclusion

This paper has proposed a SMD which assists sit-to-stand and stand-to-sit postural transitions and standing posture maintenance, as well as hands-free navigation in standing posture, for those with motor disability in the lower limbs. The SMD consists of a passive exoskeleton and electrically driven wheels. Through several assessments of the developed prototype, we confirmed the advantage of the proposed approach. The developed SMD can maintain the posture of a user and assist postural transition between the sitting and standing postures. The transition motion can be controlled by a user's anteroposterior tilting of the trunk. The exoskeleton for postural assistance is composed of passive gas-springs and a rigid link structure without electric actuators or controllers, which keeps the system small, lightweight, and low cost. Each of the ankle and knee joints of the exoskeleton is driven by a pair of gas springs.

Voluntary control of postural transition is achieved by having the user tilt the trunk anteroposteriorly. To achieve this function, the generated moment by the springs has to be within the range of the loaded moment which the user can apply by tilting the trunk. For this reason, specification of the gas springs and their attached position on the exoskeleton have to be carefully chosen according to the user's weight, height and style of postural transition. This is a complicated multiple factor exploration problem and might possibly severely affect the design workload. To mitigate the problem, we have proposed in this paper to automatically process the procedure by implementing a formalized algorithm. By using the proposed algorithm, the design workload and development time are significantly reduced. In addition, it facilitates developing of variation of the SMD for various users of various body weight, height and postural transition style. Since the proposed mechanism is scalable, future possibility includes development of a smaller version of the SMD for lightweight users, e.g., children, without compromising on any feature.

During hands-free locomotion in standing posture, a pair of in-wheel electric motors attached on the sides of the exoskeleton

is controlled according to the attitude of the trunk. The SMD is moved forward according to anterior bending motion of the trunk and is also turned according to twisting of the trunk.

The developed SMD is tailor-made for a specific subject. In the future, the configuration and interface of the SMD will be improved to accommodate users with motor dysfunction of greater variety and severity by extending the knowledge gained through this study. Recently, through some pilot experiments with several SCI users, we found that improvement of assistance on the lower part of the upper body may be helpful in some cases. Further investigation will include consideration on the fitting of the exoskeleton on to the human body, application of recently proposed ideas of self-adjusting fitting mechanisms [28], [29], the required time to get familiarized with the SMD, the easiness of wearing it on and off, modification of the structure to allow a user to sit on any chair or bed without structural interference, the effect of appearance and size of the SMD on facilitation of communication, evaluation and improvement of stability of the SMD especially when negotiating slopes, and application to people with greater variety of lower limb motor dysfunction.

REFERENCES

[1] National Spinal Cord Injury Statistical Center, "Spinal cord injury facts and figures at a glance," *J. Spinal Cord Med.*, vol. 35, no. 6, pp. 480–481, 2012.

[2] T. Hayashi, H. Kawamoto, and Y. Sankai, "Control method of robot suit HAL working as operator's muscle using biological and dynamical information," in *Proc. IEEE/RSJ Int. Conf. Intell. Robots Syst.*, 2005, pp. 3063–3068.

[3] L. Mertz, "The next generation of exoskeletons: Lighter, cheaper devices are in the works," *IEEE Pulse*, vol. 3, no. 4, pp. 56–61, Jul. 2012.

[4] H. A. Quintero, R. J. Farris, and M. Goldfarb, "A method for the autonomous control of lower limb exoskeletons for persons with paraplegia," *J. Med. Devices*, vol. 6, no. 4, pp. 0410031–0410036, Dec. 2012.

[5] G. Zeilig, H. Weingarden, M. Zwecker, I. Dudkiewicz, A. Bloch, and A. Esquenazi, "Safety and tolerance of the ReWalk exoskeleton suit for ambulation by people with complete spinal cord injury: A pilot study," *J. Spinal Cord Med.*, vol. 35, no. 2, pp. 96–101, Mar. 2012.

[6] S. Banala *et al.*, "Gravity-balancing leg orthosis and its performance evaluation," *IEEE Trans. Robot.*, vol. 22, no. 6, pp. 1228–1239, Dec. 2006.

[7] Y. Mori, K. Takayama, and T. Nakamura, "Development of straight style transfer equipment for lower limbs disabled," in *Proc. IEEE Int. Conf. Robot. Autom.*, 2004, vol. 3, pp. 2486–2491.

[8] G. Barbareschi, R. Richards, M. Thornton, T. Carlson, and C. Holloway, "Statically vs dynamically balanced gait: Analysis of a robotic exoskeleton compared with a human," in *Proc. IEEE Int. Conf. Eng. Med. Biology Soc.*, Aug. 2015, pp. 6728–6731.

[9] N. Mairs, *Waist-High in the World: A Life among the Nondisabled*. Boston, MA, USA: Beacon, 1997.

[10] T. Ito, Y. Higuchi, and H. Kimura, "Training and fitness for walking," *J. Clinical Rehabil.*, vol. 11, no. 3, pp. 204–211, 2002.

[11] A. Tsukahara, R. Kawanishi, Y. Hasegawa, and Y. Sankai, "Sit-to-stand and stand-to-sit transfer support for complete paraplegic patients with robot suit HAL," *Adv. Robot.*, vol. 24, no. 11, pp. 1615–1638, 2010.

[12] R. Kamnik and T. Bajd, "An assistive rehabilitative device for training and assessment," *J. Med. Eng. Technol.*, vol. 28, no. 2, pp. 74–80, 2004.

[13] L. Saint-Bauzel, V. Pasqui, and I. Monteil, "A reactive robotized interface for lower limb rehabilitation: Clinical results," *IEEE Trans. Robot.*, vol. 25, no. 3, pp. 583–592, Jun. 2009.

[14] Y. Morita, D. Chugo, Y. Sakaida, S. Yokota, and K. Takase, "Standing motion assistance on a robotic walker based on the estimated patient's load," in *Proc. IEEE Int. Conf. Biomed. Robot. Biomechatron.*, 2012, pp. 1721–1726.

[15] A. Fattah, S. K. Agrawal, G. Catlin, and J. Hamnett, "Design of a passive gravity-balanced assistive device for sit-to-stand tasks," *J. Mech. Des.*, vol. 128, pp. 1122–1129, 2005.

[16] LEVO AG, "Levo: Products," [Online]. Available: http://www.levo.ch/en/products.html. Accessed on: Feb. 2015.

[17] Superior Sweden AB, "Superior ME," [Online]. Available: http://superiorstanding.mamutweb.com/subdet1.htm. May 2018.

[18] UPnRIDE Robotics Ltd., "UPnRIDE," Jul. 2017. [Online]. Available: http://upnride.com

[19] Matia Robotics, Inc., "TekRMD," Jul. 2017. [Online]. Available: http://www.matiarobotics.com

[20] K. T. Ulrich, "Estimating the technology frontier for personal electric vehicles," *Transp. Res. Part C: Emerging Technol.*, vol. 13, pp. 448–462, 2005.

[21] H. G. Nguyen *et al.*, "Segway robotic mobility platform," in *Proc. SPIE*, vol. 5609, pp. 207–220, 2004.

[22] Toyota Motor Corp., "Toyota develops personal transport assistance robot 'winglet'," http://www.toyota.co.jp/en/news/08/0801_1.html, Aug. 2008.

[23] Y. Eguchi, H. Kadone, and K. Suzuki, "Standing mobility vehicle with passive exoskeleton assisting voluntary postural changes," in *Proc. IEEE/RSJ Int. Conf. Intell. Robots Syst.*, Nov. 2013, pp. 1190–1195.

[24] H. Matsui, *Motion and Body Center of Gravity*. Tokyo, Japan: Kyorin-Shoin, 1958, pp. 32–33.

[25] I. Iturrate, J. Antelis, A. Kubler, and J. Minguez, "A noninvasive brain-actuated wheelchair based on a p300 neurophysiological protocol and automated navigation," *IEEE Trans. Robot.*, vol. 25, no. 3, pp. 614–627, Jun. 2009.

[26] K. Tanaka, K. Matsunaga, and H. Wang, "Electroencephalogram-based control of an electric wheelchair," *IEEE Trans. Robot.*, vol. 21, no. 4, pp. 762–766, Aug. 2005.

[27] M. Kouchi and M. Mochimaru, *AIST/HQL Database of Human Body Dimension and Shape 2003 (H18PRO-503)*. Tokyo, Japan, National Institute of Advanced Industrial Science and Technology, 2006.

[28] M. Cempini, S. De Rossi, T. Lenzi, N. Vitiello, and M. Carrozza, "Self-alignment mechanisms for assistive wearable robots: A kinetostatic compatibility method," *IEEE Trans. Robot.*, vol. 29, no. 1, pp. 236–250, Feb. 2013.

[29] N. Jarrasse and G. Morel, "Connecting a human limb to an exoskeleton," *IEEE Trans. Robot.*, vol. 28, no. 3, pp. 697–709, Jun. 2012.

Yosuke Eguchi received the B.Eng. and M.Eng. degrees in systems and information engineering from the University of Tsukuba, Tsukuba, Japan, in 2013 and 2015, respectively.

His research interests include development of innovative mechanical systems for wearable assistive devices to enhance mobility of patients with motor impairment.

Hideki Kadone received the Ph.D. degree in information science and technology from the University of Tokyo, Japan, in 2008.

He is currently an Assistant Professor with the Center for Innovative Medicine and Engineering, and Center for Cybernics Research, University of Tsukuba, Tsukuba, Japan. His research interests include clinical motion measurement and analysis and development of wearable assistive devices to compensate for, support or improve motor function of patients after neurological or mechanical disorders.

Kenji Suzuki (M'98) received the Ph.D. degree in pure and applied physics from Waseda University, Tokyo, Japan, in 2003.

He is currently a full Professor with the Center for Cybernics Research and the principal investigator of Artificial Intelligence Laboratory, University of Tsukuba, Tsukuba, Japan. His research interests include wearable robotics and devices, affective computing, social robotics, and assistive robotics. He is a member of ACM.